Dynamics and Spatial Order of Cold Cesium Atoms in a Periodic Optical Potential

P. Verkerk, B. Lounis, C. Salomon, and C. Cohen-Tannoudji
Collège de France et Laboratoire de Spectroscopie Hertzienne de l'Ecole Normale Superieure, 24 rue Lhomond, F-75231 Paris, CEDEX 05, France

J.-Y. Courtois and G. Grynberg
Laboratoire de Spectroscopie Hertzienne de l'Ecole Normale Superieure, Université Pierre et Marie Curie, F-75252 Paris, CEDEX 05, France
(Received 23 March 1992)

The spatial distribution and the dynamics of Cs atoms in a 1D optical molasses are probed by measuring the absorption (or amplification) spectrum of a weak laser beam. Narrow (35–50 kHz) Raman lines give access for the first time to the frequency and to the damping of the atom's oscillation in the potential wells associated with light shifts. A narrower (8 kHz) Rayleigh resonance demonstrates the existence of a large-scale spatial order of the atoms, presenting some analogy with an antiferromagnetic medium.

PACS numbers: 32.80.Pj, 42.65.−k

Laser cooling is a very active subject in atomic physics [1]. Atoms confined in optical molasses have been cooled to microkelvin temperatures [2], providing an important test of the proposed polarization-gradient cooling mechanisms [3]. Theoretically, two 1D laser configurations have been studied in detail, the σ^+-σ^- and lin⊥lin configurations, where the two counterpropagating laser beams have, respectively, orthogonal circular and linear polarizations [3]. A full quantum treatment has been also performed for the lin⊥lin configuration, which predicts that the periodic character of the potentials associated with light shifts leads to vibrational levels for the atomic center of mass exhibiting a band structure [4]. The present Letter reports novel experiments using stimulated Raman and Rayleigh spectroscopy for probing the position distribution of the atoms in the light field and the dynamics of their motion. We measure for the first time the oscillation frequency of the atoms in the light potential. From the width of the Raman lines, we deduce the damping time of this oscillation, which exhibits a dramatic lengthening due to the spatial confinement of atoms to a fraction of optical wavelength (Lamb-Dicke effect) [5]. Furthermore, we get stimulated Rayleigh signals which give experimental evidence for a large-scale spatial order of the atomic gas presenting some analogy with an antiferromagnetic medium.

Contrary to previous work investigating Raman transitions for atoms in a 3D magneto-optical trap [6,7], we restrict ourselves to a 1D optical molasses of adjustable polarization state. This molasses is obtained as follows: Cesium atoms are cooled and trapped by three pairs of σ^+-σ^- counterpropagating beams in a magneto-optical trap. After this loading and cooling phase the inhomogeneous magnetic field is switched off and the intensity of each trapping beam is reduced from 5 mW/cm^2 to about 0.1 mW/cm^2. A pump wave of frequency ω made of two counterpropagating beams having σ^+-σ^- or linear crossed polarizations (lin⊥lin) is then switched on. A 1D molasses is achieved in a transient way (the atomic density decreases with a time constant of 5–50 ms because of the transverse heating induced by the pump beams). We monitor the transmitted intensity of a weak traveling probe wave of frequency ω_p making a 3° angle with the pump wave. All laser beams are derived from a frequency-stabilized diode laser (jitter < 1 MHz) and are independently tuned to the red side of the $6S_{1/2}(F=4) \rightarrow 6P_{3/2}(F'=5)$ transition. Typical intensities for the pump and probe beams are, respectively, $I=5$ mW/cm^2 and $I_p=0.1$ mW/cm^2. We show in Fig. 1 the probe absorption spectrum versus ω_p for two different configurations of polarization of the pump beams. In Fig. 1(a), these beams are in the σ^+-σ^- configuration whereas in Figs. 1(b) and 1(c) they have linear orthogonal polarizations. Figure 1(b) corresponds to the probe polarization orthogonal to that of the pump wave which propagates in the same direction; in Fig. 1(c), it is parallel. The difference between Figs. 1(a) and 1(b),1(c) is striking. While the absorption varies smoothly over a range of about 500 kHz in the σ^+-σ^- case, much sharper structures are observed in the lin⊥lin case. First, one observes two narrow resonances [width ~35 kHz in Fig. 1(b) and ~50 kHz in Fig. 1(c)] symmetrically located with respect to $\omega_p=\omega$ and corresponding to extra absorption for $\omega_p-\omega>0$ and to gain for $\omega_p-\omega<0$. For a pump detuning of $\delta=-10$ MHz, the position Ω_v of the maximum of these lateral resonances varies as $I^{0.4}$. Second, spectra shown in Figs. 1(b) and 1(c) exhibit a very steep central structure which depends on the orientation of the probe polarization. The narrowest resonance [Fig. 1(c)] appears to be dispersive with a peak-to-peak separation of 8 kHz [8].

We interpret these resonances as follows. In the σ^+-σ^- case, the ground-state light shifts do not depend on space, and there are no bounds states in the optical potential. Furthermore, as shown in a preceding paper [6], the transmission probe spectrum involves on one hand Raman transitions between Zeeman sublevels which are populated differently and light shifted and on the other hand

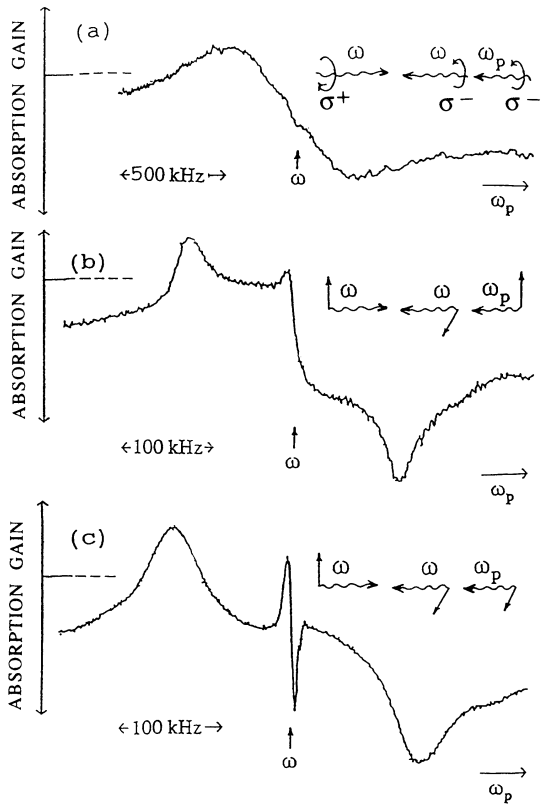

FIG. 1. Probe absorption spectrum for three different polarization configurations. (a) σ^+-σ^- polarized pump waves. The signal is 2% of the probe intensity and the shape is insensitive to the probe polarization (experimental frequency resolution of $\sim$10 kHz). (b) lin$\perp$lin polarized pump waves (probe has a linear polarization perpendicular to the polarization of the copropagating pump wave). (c) Same as (b) but with a probe polarization parallel to the one of the copropagating pump wave. In (b) and (c), the frequency resolution is $\sim$3 kHz and signals are typically 10% of the probe intensity. Note the difference of scales on the frequency axis between (a) and (b),(c).

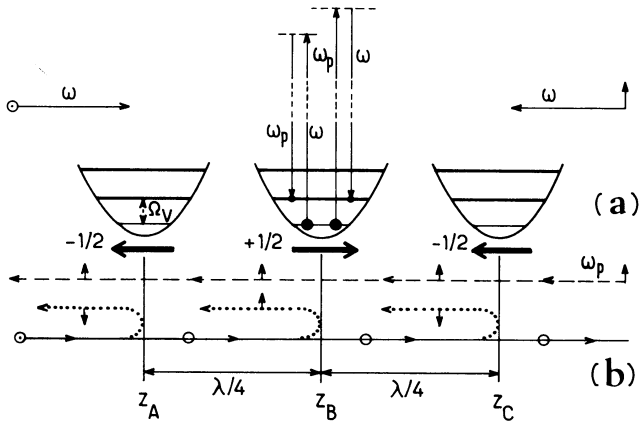

FIG. 2. (a) Bottom part of three adjacent optical potential wells for a $F=\frac{1}{2}\rightarrow F'=\frac{3}{2}$ transition in a lin$\perp$lin pump configuration. These potential wells are alternatively associated with ground-state sublevels $m_J=-\frac{1}{2}$ and $m_J=\frac{1}{2}$ as shown in the figure. The magnetizations in successive planes have opposite signs as in an antiferromagnetic medium. The vertical arrows represent Raman processes between $v=0$ and $v=1$ vibrational levels, leading to an absorption or an amplification of the probe beam. More generally, all transitions $v\rightarrow v\pm 1$ contribute to the Raman lines shown in Figs. 1(b) and 1(c) in a way which depends on the probe polarization. This explains the difference in the widths of the Raman resonances. (b) Interpretation of the central narrow structure for the configuration of Fig. 1(c). The pump beam coming from the left (solid line) is backscattered by the magnetization planes in z_A, z_B, and z_C. The backscattered waves (dotted lines) undergo a rotation of polarization and can interfere with the probe wave coming from the right (dashed line). The change of sign of the rotation of polarization due to the change of sign of the magnetization (represented by a bold arrow) compensates for the π phase shift due to propagation between successive planes.

two-wave mixing resonances [9,10]. The width of the resonances in Fig. 1(a) is on the order of the optical pumping rate (typically 0.5 MHz in our experimental conditions), which varies linearly with the laser intensity as does the peak-to-peak distance of Fig. 1(a).

In the case of crossed linear polarizations, the light shifts display a periodic spatial modulation (period $\lambda/2$). To interpret the results, we consider the simple case of a $F=\frac{1}{2}\rightarrow F'=\frac{3}{2}$ transition [4]. Each Zeeman sublevel $m_F=\pm\frac{1}{2}$ has a well-defined spatially modulated light shift as depicted in Fig. 2. Near the bottom of the potential wells the atomic medium is alternatively polarized: $\langle J_z\rangle$ changes sign every $\lambda/4$. When the light shifts are sufficiently large, several well-separated bands are predicted in the potential wells associated with the light shifts [4]. The energy separation $\hbar\Omega_v$ between two consecutive bands near the bottom of the potential is proportional to the Rabi frequency, i.e., to $\sqrt{I}$. We thus interpret the lateral resonances of Figs. 1(b) and 1(c) in terms of Raman transitions between adjacent bands as illustrated in Fig. 2. The slight discrepancy between the $I^{1/2}$ law and the experimentally observed $I^{0.4}$ law may result from a weak saturation of the atomic transition. Note that these Raman transitions involve only the atom's external degrees of freedom, within a given m_J manifold. One unexpected feature of these Raman resonances is that their width is almost 1 order of magnitude smaller than the optical pumping rate. This result is very surprising since one would expect the Raman coherence between two bands to be destroyed by an absorption-spontaneous-emission cycle. Actually, a large amount of coherence is preserved during such a cycle because of the spatial localization of atoms. An atom leaving, by absorption, a localized vibrational state with $m_F=\frac{1}{2}$ has a probability close to 1 to return to the same state. First, the probability that m_F changes is very small because the polarization of the laser field is nearly pure σ^+ for a localized $m_F=\frac{1}{2}$ state, and the absorption of a σ^+ photon

brings the atom into $m_{F'}=\frac{3}{2}$ from where it can only return to $m_F=\frac{1}{2}$. Second, the probability that the vibrational quantum number changes is also very small. More precisely, since the transfer of momentum $\hbar\Delta k$ in the scattering process is small compared to the width of the initial wave function in momentum space (because of spatial localization), the atomic state at the end of the scattering process has a very small overlap with the other vibrational wave functions (Lamb-Dicke effect). The damping rate of the coherence between two vibrational levels is thus considerably reduced because several absorption-spontaneous-emission cycles are required to destroy this coherence [11]. The localization assumption is consistent with the spatial extent $[(2\hbar/M\Omega_v)^{1/2}]$ of the ground-state wave function which is on the order of $\lambda/25$ for $\Omega_v/2\pi=120$ kHz.

We now sketch a physical interpretation of the narrow central structures of Figs. 1(b) and 1(c), by studying how the probe changes the populations of the vibrational states in each potential well and then, by considering the interference between the probe field and the field scattered from the pump beams, by these probe-induced changes of populations. Consider first the case of Fig. 1(b). In order to qualitatively understand the effect of the probe, we combine the copropagating pump beam with the probe. The resulting field is space independent and has a time-dependent polarization which has alternatively a dominant σ^+ or σ^- component, the period being $2\pi/|\omega-\omega_p|$. When the dominant component is σ^+ polarized, optical pumping redistributes the atomic population between the various vibrational states and results in a global departure from the potential wells associated with $m_F=-\frac{1}{2}$ towards those corresponding to $m_F=+\frac{1}{2}$. This optical pumping gives rise to a net magnetization along Oz (i.e., with a nonzero spatial integral), which is modulated at $|\omega-\omega_p|$ and which is phase shifted with respect to the exciting field because the response times of the populations of the various vibrational levels are nonzero. Consider now the effect of such a modulated magnetization on the pump beam ω copropagating with the probe. The polarization of the pump beam undergoes a modulated Faraday rotation, so that the transmitted pump beam has a small component having the same polarization (and also the same frequency ω_p and direction of propagation) as the probe beam and can thus interfere with it [12]. As shown in [10], the energy transfer from the pump beam to the probe beam or vice versa varies with $\omega_p-\omega$ as a dispersion curve with extrema for $|\omega-\omega_p|\simeq 1/\tau$, where τ is the response time of the populations. The interference process considered here involves a forward scattering of the pump wave, so that all population changes in all vibrational levels are probed. Several different response times are thus involved and the central structure results from the superposition of several dispersion curves with different widths, which explains its uncommon shape.

We consider now the case of Fig. 1(c). As above, we combine the copropagating pump beam with the probe. The resulting field has then a fixed linear polarization but its intensity is modulated. When this intensity is maximum, the resulting field adds everywhere an equal amount of σ^+ and σ^- light. The transfers due to optical pumping between the potential wells associated with $m_F=\pm\frac{1}{2}$ balance each other and no net magnetization appears in the sample. The only effect of the probe is to change the population of each vibrational state, the total population in each potential well remaining the same. These population changes are modulated at $|\omega-\omega_p|$ and phase shifted with respect to the exciting field. We now analyze the effect on the pump beams of the population redistribution between the vibrational levels. We have represented in Fig. 2 three successive potential wells corresponding to $m_F=-\frac{1}{2}$, $m_F=+\frac{1}{2}$, and $m_F=-\frac{1}{2}$, located, respectively, at z_A, z_B, and z_C with $z_B-z_A=z_C-z_B=\lambda/4$. The pump beam coming from the left is backscattered by the magnetization associated with the atoms occupying the potential well in $z=z_A$. The backscattered wave undergoes a change of polarization and a change of frequency, so that it has a component having the same polarization, the same frequency, and the same direction of propagation as the probe beam coming from the right. We now show that the waves backscattered by the magnetization planes in $z=z_A$, $z=z_B$,... interfere constructively. The phase shift due to the propagation between the waves backscattered in z_A and z_B is equal to π, since $z_B-z_A=\lambda/4$. However, the magnetizations in two successive planes $z=z_A$ and $z=z_B$ are opposite (as in an antiferromagnetic medium), so that the rotation of the polarization has an opposite sign in $z=z_A$ and $z=z_B$ (see Fig. 2) and this change of sign compensates for the π phase shift due to propagation. The interference of the total backscattered wave with the probe wave gives rise to a two-wave mixing signal which has a dispersion shape and a width corresponding to the inverse of the response time of the involved vibrational levels. So far, we have considered only magnetization planes. The wave functions of the vibrational levels have actually a certain width δz along Oz. If δz is too large, the waves backscattered by the right part and the left part of the wave function interfere destructively. This shows that the two-wave mixing signal will come predominantly from the localized vibrational levels. The observation of such a signal is thus a direct evidence for a spatial order of the atoms. Since the time required to reach the population equilibrium for these localized levels is very long (because of the Lamb-Dicke effect), one understands why the central structure of Fig. 1(c) is so narrow [13].

Our qualitative interpretations are supported by a calculation of the probe absorption spectrum, based on the formalism of [4]. Theoretical spectra, in reasonable agreement with those of Fig. 1, will be reported in a forthcoming publication. We conclude this Letter by

summarizing the information contained in the spectra of Figs. 1(b) and 1(c). The position of the Raman sidebands gives the oscillation frequency of the atom in the optical potential wells of Fig. 2. The narrow width of these sidebands, in comparison with the width observed when atoms are not localized [Fig. 1(a)], is a clear evidence for a lengthening of the dephasing time of the atom oscillatory motion due to the Lamb-Dicke effect. The very narrow central structure of Fig. 1(c) is due to a backward Bragg diffraction of one of the two pump beams by a large-scale spatially ordered structure consisting of equidistant sets of localized atoms, separated by $\lambda/4$, the magnetizations in two successive sets being opposite, as in an antiferromagnetic medium.

We are grateful to J. Dalibard and Y. Castin for fruitful discussions. Laboratoire de Spectroscopie Hertzienne is a unité de recherche de l'Ecole Normale Supérieure et de l'Université Pierre et Marie Curie, associée au CNRS. This work has been supported by DRET (No. 89214) and CNES (No. 910414).

[1] See, for example, *Laser Manipulation of Atoms and Ions*, edited by E. Arimondo and W. D. Phillips, Varenna Summer School, 1991 (North-Holland, Amsterdam, 1992).

[2] C. Salomon, J. Dalibard, W. D. Phillips, A. Clairon, and S. Guellati, Europhys. Lett. **12**, 683 (1990); C. Monroe, W. Swann, H. Robinson, and C. Wieman, Phys. Rev. Lett. **65**, 1571 (1990).

[3] J. Dalibard and C. Cohen-Tannoudji, J. Opt. Soc. Am. B **6**, 2023 (1989); P. J. Ungar, D. S. Weiss, E. Riis, and S. Chu, J. Opt. Soc. Am. B **6**, 2058 (1989); C. Cohen-Tannoudji and W. D. Phillips, Phys. Today **43**, No. 10, 33 (1990).

[4] Y. Castin and J. Dalibard, Europhys. Lett. **14**, 761 (1991).

[5] Localization of atoms in wavelength-size potentials has been observed in 3D molasses by C. I. Westbrook, R. N. Watts, C. E. Tanner, S. L. Rolston, W. D. Phillips, P. D. Lett, and P. L. Gould, Phys. Rev. Lett. **65**, 33 (1990), and by N. P. Bigelow and M. G. Prentiss, Phys. Rev. Lett. **65**, 29 (1990).

[6] D. Grison, B. Lounis, C. Salomon, J.-Y. Courtois, and G. Grynberg, Europhys. Lett. **15**, 149 (1991).

[7] J. W. R. Tabosa, G. Chen, Z. Hu, R. B. Lee, and H. J. Kimble, Phys. Rev. Lett. **66**, 3245 (1991).

[8] The widths of these resonances are much narrower than the laser jitter. This is not surprising because they correspond to Raman or Rayleigh processes which involve frequency differences between two sources derived from the same laser. The relative frequency jitter of the two sources has been independently measured to be less than 0.2 kHz.

[9] G. Grynberg, E. Le Bihan, and M. Pinard, J. Phys. (Paris) **47**, 1321 (1986).

[10] G. Grynberg, M. Vallet, and M. Pinard, Phys. Rev. Lett. **65**, 701 (1990).

[11] When increasing the pump intensity I, the optical pumping rate increases but the localization becomes more pronounced. This is why the width of the Raman resonances grows with I more slowly than the optical pumping rate, as observed experimentally.

[12] The fact that the experiment is made with a small angle between the probe and pump beams does not invalidate this explanation. The important point is that the scattering of the pump wave on the induced magnetization creates a wave which does propagate in the probe direction. See [9].

[13] The previous analysis considered only the scattering of one of the two pump beams by a modulated magnetization. Other scattering processes should also be included to fully describe the central resonances. For example, in the configuration of Fig. 1(b), the $m_F = -\frac{1}{2}$ and $m_F = \frac{1}{2}$ potential wells are alternatively depleted. The backscattering of the counterpropagating pump beam by such a population grating gives rise to a wave that can interfere with the probe wave and thus yields other two-wave mixing contributions to the central resonance. More generally, for angular momenta in the ground state higher than $\frac{1}{2}$, one should also consider the effect of a modulated alignment.